



Synthesis and characterization of Ru(IV) and Rh(I) complexes containing phenylimidazole ligands

Rakesh Kumar Gupta^a, Ashish Kumar Singh^a, Mahendra Yadav^a, Prashant Kumar^a, Sanjay Kumar Singh^b, Peizhou Li^b, Qiang Xu^b, Daya Shankar Pandey^{a,*}

^a Department of Chemistry, Faculty of Science, Banaras Hindu University, Varanasi 221 005, Uttar Pradesh, India

^b National Institute of Advanced Industrial Science and Technology (AIST), 1-8-31 Midorigaoka, Ikeda, Osaka 563-8577, Japan

ARTICLE INFO

Article history:

Received 28 February 2010

Received in revised form

17 April 2010

Accepted 19 April 2010

Available online 7 May 2010

Keywords:

Ru(IV)

Rh(I)

1-(4-cyanophenyl)imidazole

1-(4-nitrophenyl)imidazole

1-(4-formylphenyl)imidazole

1-(4-hydroxyphenyl)imidazole

DFT

ABSTRACT

The reactions of chloro-bridged dimeric complexes $[\{(\eta^3;\eta^3\text{-C}_{10}\text{H}_{16})\text{Ru}(\mu\text{-Cl})\text{Cl}\}_2]$ and $[\{(\eta^4\text{-C}_8\text{H}_{12})\text{RhCl}\}_2]$ with 1-(4-cyanophenyl)imidazole (CPI), 1-(4-nitrophenyl)imidazole (NOPI), 1-(4-formylphenyl)imidazole (FPI) and 1-(4-hydroxyphenyl)imidazole (HPI) have been investigated. These reactions afforded complexes with the general formulations $[\{(\eta^3;\eta^3\text{-C}_{10}\text{H}_{16})\text{RuCl}_2(\text{L})\}]$ (L = CPI, **1**; NOPI, **2**; FPI, **3**; HPI, **4**) and $[\{(\eta^4\text{-C}_8\text{H}_{12})\text{RhCl}(\text{L})\}]$ (L = CPI, **5**; NOPI, **6**; FPI, **7**; HPI, **8**). Resulting complexes have been characterized by analytical and spectral (IR, ¹H and ¹³C NMR, UV–Vis) studies. Crystal structures of **2**, **5** and **6** have been determined by single crystal X-ray diffraction analyses. Structural studies on the complexes **2**, **5** and **6** revealed the presence of extensive inter- and intra-molecular C–H⋯X (X = O and Cl) and C–H⋯π interactions. Theoretical studies have been performed to authenticate the structures and NBO calculations to determine electronic properties of the complexes.

© 2010 Elsevier B.V. All rights reserved.

1. Introduction

The chloro-bridged dimeric ruthenium(IV) and rhodium(I) complexes $[\{(\eta^3;\eta^3\text{-C}_{10}\text{H}_{16})\text{Ru}(\mu\text{-Cl})\text{Cl}\}_2]$ and $[\{(\eta^4\text{-C}_8\text{H}_{12})\text{RhCl}\}_2]$ are known for many years [1,2]. However, their chemistry has not been developed to the same extent as that of chloro-bridged dimeric arene ruthenium $[\{(\eta^6\text{-arene})\text{Ru}(\mu\text{-Cl})\text{Cl}\}_2]$ [(arene = benzene and its derivatives) and pentamethylcyclopentadienyl rhodium and iridium complexes $[\{(\eta^5\text{-C}_5\text{Me}_5)\text{M}(\mu\text{-Cl})\text{Cl}\}_2]$ (M = Rh, Ir) [3–8]. Like arene ruthenium and pentamethylcyclopentadienyl rhodium/iridium complexes these undergo chloro-bridge cleavage reactions leading to the formation of neutral and cationic mononuclear complexes [9–11]. Such complexes have been important because of their involvement in a number of stoichiometric and catalytic reactions including reduction of carbonyl group, activation of carbon-hydrogen bonds, alkene oligomerization and polymerizations [12–15].

The designing and syntheses of novel coordination ligands are challenging and continuous efforts are being made to tune the

nature of interactions between the reactants to afford desired structures [16–21]. In this context, imidazole and its derivatives are particularly interesting because of their excellent ligational properties and diverse coordination modes [22–26]. Cyanide is another ligand that has attracted immense current attention and employed in the construction of extended structures [27–29]. Further, ligands containing both the imidazole and cyanide group have scarcely been utilized in the construction of functional MOFs [30]. 1-(4-cyanophenyl)imidazole (CPI) and related ligands like 1-(4-nitrophenyl)imidazole (NOPI), 1-(4-formylphenyl)imidazole (FPI) and 1-(4-hydroxyphenyl)imidazole (HPI), are known for many years [31–35]. While we and other research groups have reported numerous mono- and binuclear compounds containing CPI, the ligational properties of NOPI, FPI and HPI with the complexes $[\{(\eta^3;\eta^3\text{-C}_{10}\text{H}_{16})\text{Ru}(\mu\text{-Cl})\text{Cl}\}_2]$ and $[\{(\eta^4\text{-C}_8\text{H}_{12})\text{RhCl}\}_2]$ have not been studied [31–33,36,37].

To develop the chemistry of ligands CPI, NOPI, FPI and HPI and because of our interests in this area we have examined reactivity of with the dimeric complexes $[\{(\eta^3;\eta^3\text{-C}_{10}\text{H}_{16})\text{Ru}(\mu\text{-Cl})\text{Cl}\}_2]$ and $[\{(\eta^4\text{-C}_8\text{H}_{12})\text{Rh}(\mu\text{-Cl})\}_2]$ with these ligands and have isolated a series of neutral mononuclear complexes. In this paper we report the synthesis and spectral characterization of complexes containing

* Corresponding author. Tel.: +91 542 6702480; fax: +91 542 2368174.
E-mail address: dspbhu@bhu.ac.in (D.S. Pandey).

CPI, NOPI, FPI and HPI and $\{(\eta^3;\eta^3\text{-C}_{10}\text{H}_{16})\text{RuCl}_2\}/\{(\eta^4\text{-C}_8\text{H}_{12})\text{RhCl}\}$ -moieties. Also, we present herein the crystal structures of representative complexes $[(\eta^3;\eta^3\text{-C}_{10}\text{H}_{16})\text{RuCl}_2(\text{NOPI})]$, $[(\eta^4\text{-C}_8\text{H}_{12})\text{RhCl}(\text{CPI})]$ and $[(\eta^4\text{-C}_8\text{H}_{12})\text{RhCl}(\text{NOPI})]$ and theoretical studies performed on these complexes to investigate their electronic properties.

2. Result and discussion

2.1. Synthesis and characterization

The chloro-bridged dimeric complexes $\{[(\eta^3;\eta^3\text{-C}_{10}\text{H}_{16})\text{Ru}(\mu\text{-Cl})\text{Cl}]_2\}$ and $\{[(\eta^4\text{-C}_8\text{H}_{12})\text{Rh}(\mu\text{-Cl})\text{Cl}]_2\}$ reacted with 1-(4-cyanophenyl)imidazole (CPI), 1-(4-nitro-phenyl)imidazole (NOPI), 1-(4-formylphenyl)imidazole (FPI) and 1-(4-hydroxy-phenyl)-imidazole (HPI) in dichloromethane under stirring conditions at room temperature to afford mononuclear complexes $[(\eta^3;\eta^3\text{-C}_{10}\text{H}_{16})\text{RuCl}_2(\text{L})]$ (L = CPI, **1**; NOPI, **2**; FPI, **3**; HPI, **4**) and $[(\eta^4\text{-C}_8\text{H}_{12})\text{RhCl}(\text{L})]$ (L = CPI, **5**; NOPI, **6**; FPI, **7**; HPI, **8**) in reasonably good yields. A simple scheme showing the synthesis of complexes is depicted in Scheme 1.

The complexes **1–8** are non-hygroscopic, air-stable crystalline solids soluble in common organic solvents viz., dichloromethane, chloroform, acetone, acetonitrile, DMSO, DMF and insoluble in water, methanol, diethyl ether, petroleum ether, *n*-hexane, benzene and toluene. Analytical and spectral data (IR, ^1H and ^{13}C NMR and electronic absorption and emission) provided valuable information about the composition and structure of the complexes.

IR spectra of the complexes under study displayed shifts in the position of bands associated with $\nu(\text{C}=\text{N})$ of imidazole by $\sim 10\text{--}20\text{ cm}^{-1}$, (1605, **1**; 1599, **2**; 1602, **3**; 1604, **4**; 1598, **5**; 1598, **6**; 1596, **7** and 1602 cm^{-1} , **8**) in comparison to the uncoordinated ligands (1615, CPI; 1620, NOPI; 1617, FPI and 1620 cm^{-1} , HPI) [31,34,35]. It suggested the linkage of ligands to metal centre through imine nitrogen of imidazole. Characteristic bands corresponding to the $\nu(\text{C}\equiv\text{N})$, $\nu(\text{NO}_2)$, $\nu(\text{C}=\text{O})$ and $\nu(\text{O}-\text{H})$ group of CPI, NOPI, FPI, and HPI vibrated at 2230, 1515, 1336, 1698 and 3600 cm^{-1} in the IR spectra of respective complexes [31,34,35].

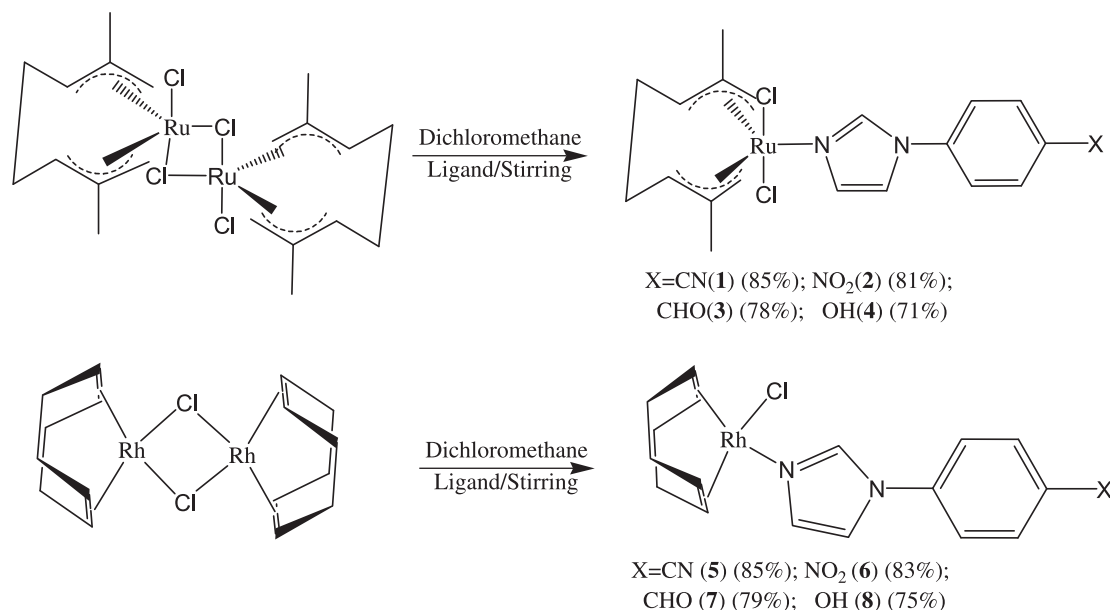
2.2. NMR spectral studies

^1H NMR spectral data of the complexes corroborated well with the proposed formulations. Notably, the protons associated with ligands and precursor complexes resonated at almost the same position in the ^1H NMR spectra of respective complexes. For example, **1–4** in its spectrum displayed resonances due to 2,7-dimethyloctadienediyl ($\eta^3;\eta^3\text{-C}_{10}\text{H}_{16}$) protons at ~ 2.40 (CH_3 protons), 3.10 (CH_2 protons), 4.40, 4.60, and 5.20 ppm (bis-allyl), while protons associated with 1,4-cyclooctadiene ($\eta^4\text{-C}_8\text{H}_{12}$) in **5–8** resonated at ~ 1.90 (CH_2 protons), 2.50 (CH_2 protons), 4.50 (for $-\text{CH}$ protons) ppm [38–40]. One can see that there is an insignificant shift in the position of various signals corresponding to 2,7-dimethyloctadienediyl ($\eta^3;\eta^3\text{-C}_{10}\text{H}_{16}$) or 1,4-cyclooctadiene ($\eta^4\text{-C}_8\text{H}_{12}$) protons. On the other hand, resonances associated with the aromatic proton of ligands appeared between $\sim 7.2\text{--}8.8$ ppm [31,34,35]. Diagnostic signals due to the aldehydic protons in **3** and **7** appeared at ~ 10.00 ppm [35], while phenolic protons in **4** and **8** resonated at ~ 8.8 ppm. The position of resonances associated with various protons and area under each peak in the ^1H NMR spectra of respective complexes corroborated well with the proposed formulations.

^{13}C NMR spectra of the complexes displayed an analogous pattern of resonances, supporting the proposed formulations. Resulting data is summarized in the experimental section and representative spectra for **2**, **5** and **6** are shown in Figs. S1–S3. The ^{13}C NMR spectra of **1–4** exhibited resonances corresponding to $\eta^3;\eta^3\text{-C}_{10}\text{H}_{16}$ carbons at 21.10 (CH_3), 36.89 (CH_2), and 77.81, 95.25, 133.45 (C, bis-allyl) ppm [38], while **5–8** displayed signals associated with $\eta^4\text{-C}_8\text{H}_{12}$ carbons at 30.75 (CH_2), 79.62 (CH) ppm [39,40]. The carbons of $-\text{CHO}$ and $-\text{C}=\text{N}$ resonated at ~ 217 and ~ 112 ppm, respectively. The resonances associated with other carbons of the ligands were displayed in the range of $\sim 112\text{--}150$ ppm [31,35].

2.3. Electronic absorption spectral studies

The oxidation state of metal centre ruthenium in complexes **1–4** is (+IV, d^4) and geometry is trigonal bipyramidal (TBP). In these



Scheme 1. Synthesis of the complexes **1–8**.

complexes there is no peak corresponding either to metal centre ($d-d$ transition) or the one involving metal centre (LMCT or MLCT) [41]. The electronic spectra of these complexes displayed only intra-ligand transitions suggesting that the electronic absorption spectroscopy is not a good tool to follow the formation of this type of complexes. However, in the case of **5–8** remarkable changes in the colour of resulting complexes have been observed along the ligand series. It provided clear evidence about changes in the electronic level of the metal with a change in the ligands. It is noteworthy that the difference in colour of complexes depend on substituents $-X$ of the ligands ($X = \text{CN}$, yellow; NO_2 , orange; CHO , light yellow; OH , yellow). Electronic absorption spectra of the complexes displayed weak and broad bands at ~ 600 nm, broad bands in the region 374–380 nm (Fig. 1) and intense bands at ~ 261 –292 nm. The bands at ~ 600 nm have been assigned to the $d-d$ transitions. The extinction coefficients ($\sim 100 \text{ L mol}^{-1} \text{ cm}^{-1}$) are high, considering that the transition is spin-forbidden for d^8 configuration of Rh(I), but there is a relaxation of the selection rule due to spin-orbit coupling usually observed with the heavy d -metals complexes [42].

2.4. X-ray crystallography

Molecular structures of **2**, **5** and **6** have been determined crystallographically. Details about the data collection, solution and refinement is summarized in the crystallographic section, selected geometrical parameters are gathered in Tables S1–S2 and ORTEP views (30% probability of thermal ellipsoid) are depicted in Figs. 2–4. The asymmetric unit of **2** contains two independent molecules which are essentially identical (Table S1). Coordination geometry about ruthenium centre is distorted trigonal bipyramidal (TBP) wherein, equatorial positions are occupied by the allyl groups of ($\eta^3, \eta^3\text{-C}_{10}\text{H}_{16}$)- and the N1 from NOPI, while axial ones by the chloro groups C11 and C12 [43,44]. The allyl groups are η^3 -bonded to ruthenium with Ru–C bond distances in the range of 2.240(3)–2.286(3) Å. The C–C distances and internal C–C–C bond angles within the allyl groups are 1.40 and 1.41 Å (mean) and 116.0 and 115.6° (mean) for the first and second molecule, respectively [43,44]. These are consistent with the reported values in other transition metal η^3, η^3 -2,7-dimethyloctadienediyl complexes.

Methyl substituents C(9)/C(10) and C(28)/C(29) exhibited deviation from the allyl planes towards the ruthenium centre by 1.8 and 2.0° in first and 2.1 and 1.9° in the second molecule. This

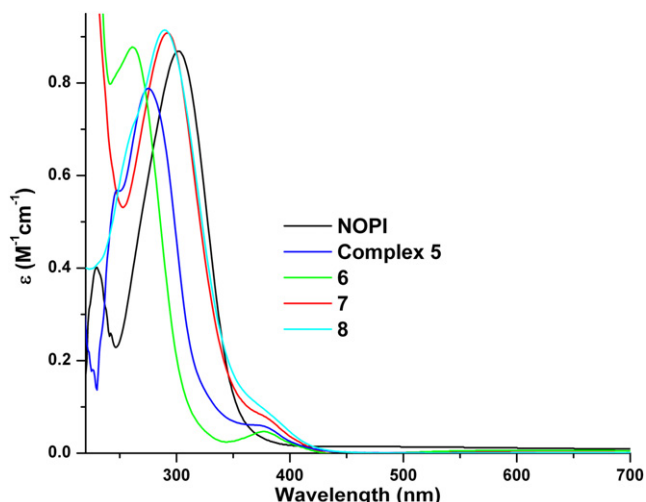


Fig. 1. UV–Vis spectra of complex **5–8**.

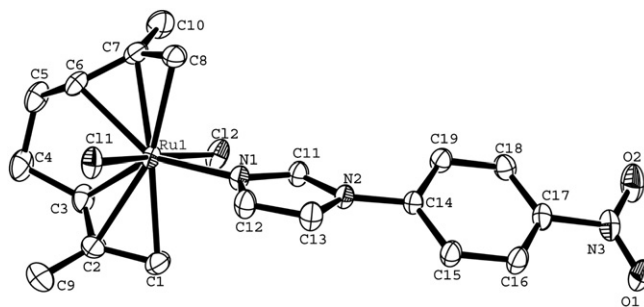


Fig. 2. Crystal structure of **2** at 30% probability of thermal ellipsoids. (H atoms excluded for clarity).

observation is consistent with earlier reports [43,44]. The Ru(1)–Cl(1) and Ru(1)–Cl(2) bond distances are 2.4384(8) and 2.4138(8) Å while, Ru(2)–Cl(3) and Ru(2)–Cl(4) are 2.4427(8) and 2.4108(8) Å, respectively [45–48]. These distances are comparable to the Ru–Cl distances in other related systems. The Ru–N bond distance of 2.175(2) Å is comparable to the values reported in literature [49–51].

The common structural feature of complexes **5** and **6** is the square planar arrangement of various groups about metal centre rhodium. The asymmetric unit of **6** contains two molecules, while only one molecule is present in **5**. Arrangement of the various groups about rhodium in both the complexes are analogous and completed by cyclooctadiene coordinated in η^4 -manner, the chloro group and imidazolyl nitrogen. Considering cyclooctadiene ring as occupying two sites, coordination geometry about the rhodium is square planar, which is reflected by the *cis* angles (C1–Rh–C6/C2–Rh–C5) of 81.9(2)/81.87(2)° in **5** and (C18–Rh1–C6/C2–Rh1–C5) 81.8(1)/81.82(1)° about Rh1 and (C18–Rh2–C25/C19–Rh2–C22) 81.4(1)/82.0(1)° about Rh2 in complex **6**. These are comparable to the values reported in other rhodium complexes [52]. Cyclooctadiene ring adopted a tub shaped configuration in both the complexes **5** and **6**.

It is noteworthy that, despite having different substituents on the phenyl ring of coordinated ligands CPI and NOPI, various bond lengths and angles about the rhodium exhibit insignificant differences. The ligands CPI and NOPI in these complexes occupy an equatorial position and Rh–N bond distances in **5** and **6** are 2.106(3) and 2.130(3) Å, respectively. Slightly large Rh–N distance in **6** as compared to that in **5** may be attributed to greater inductive effect of $-\text{NO}_2$. These distances are comparable to the values reported in literature [49–52]. The torsion angles between the cyanophenyl/nitrophenyl and imidazole rings in complexes **5** and **6** are 33.06 and 16.05°, respectively.

Weak interaction studies on complex **2** revealed that the C–H \cdots X (X=O, N and Cl) inter-molecular interactions (C(8)–H(8) \cdots O(1) = 3.2692 Å, C(8)–H(8) \cdots N(3) = 3.2564 Å, C(13)–H(13) \cdots

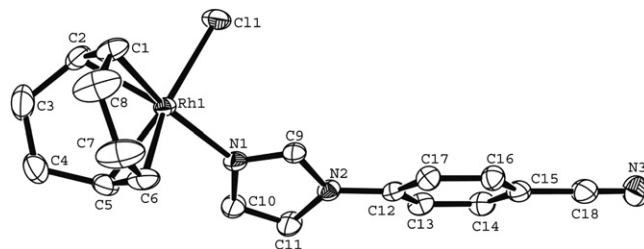


Fig. 3. Crystal structure of **5** at 30% probability of thermal ellipsoids. (H atoms omitted for clarity).

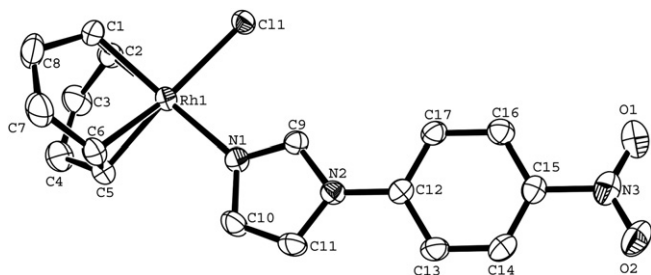


Fig. 4. Crystal structure of **6** at 30% probability of thermal ellipsoid. (H atoms omitted for clarity).

Cl(3) = 3.6078 Å, C(32)–H(32)⋯Cl(1) = 3.4816 Å [53]) leads to a layered motif (Fig. 5). Significant interaction parameters along with symmetry are listed in Table 1.

In complex **5**, hydrogen atom H6 from cyclooctadiene (η^4 -C₈H₁₂) is involved in a long range C–H⋯ π (C6–H6⋯C13) interaction with C13 of the phenyl ring (contact distance of 2.746 Å; H6 to centroid distance 3.072 Å) of CPI (Fig. S4). Similarly, in complex **6**, strong π – π interactions have been observed in both the asymmetric units, resulting in a dimeric structure, shown in Fig. 6.

Weak interaction studies on **6** further revealed that the C–H⋯X (X = N, O and Cl) interactions lead to elliptical pipe cavity along the crystallographic-*c*' axis. (Fig. 7) The major axis of the ellipse is of 5.61 Å and minor axis is 4.83 Å.

2.5. Theoretical studies

2.5.1. Geometry optimizations

Optimized geometries for the complexes is depicted in Figs. S6–S13. Optimized bond lengths and angles in **2**, **5** and **6** are in good agreement with the single crystal X-ray structural data (Tables S1 and S2). Structures of the other complexes also, have been authenticated by optimization of the expected structures and comparing the single crystal X-ray data for **2**, **5** and **6**. Frequency calculations have been performed to check whether optimised geometries were minima on the potential energy surface or not.

2.5.2. Bonding analysis

We begin with the analysis of bonding situation in the complexes with a discussion of natural atomic charges. The natural bond orbital (NBO) charge distribution in complexes **1–8** is shown below in Scheme 2.

Calculated natural population analysis (NPA) charge distributions indicated that the Ru/Rh atom (η^3 ; η^3 -C₁₀H₁₄)/(η^4 -C₈H₁₂) and ligands are positively charged, while chloro groups are negatively charged. We observed that there is analogous charge distribution in **1–4** and **5–8**. Hence, conclude that the electronic properties of **1–4** and **5–8** are similar. To visualize the Ru/Rh–N1, Ru/Rh–Cl1, Ru/Rh–

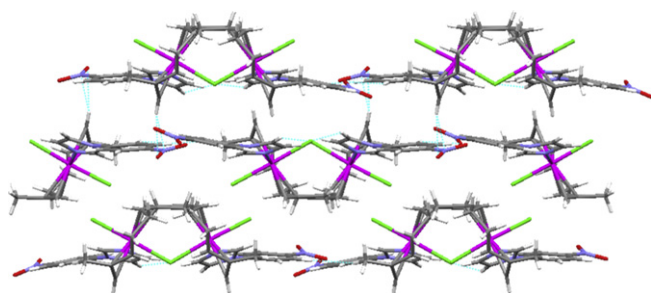


Fig. 5. Zig-Zag layered motif in **2** along crystallographic-*c*' axis.

Table 1
Matrices for weak bonding interactions in **2**, **5** and **6**

2	d(D–H) Å	d(H⋯A) Å	d(D⋯A) Å	<(DHA) ^o
C(8)–H(8)⋯O(1) ^a	0.93	2.40	3.2692	155
C(8)–H(8)⋯N(3) ^a	0.93	2.37	3.2564	159
C(13)–H(13)⋯Cl(3) ^b	0.93	2.79	3.6078	148
C(32)–H(32)⋯Cl(1) ^c	0.93	2.61	3.4816	157
5				
C(9)–H(9)⋯Cl(1) ^d	0.93	2.79	3.558	141
C(13)–H(13)⋯Cl(1) ^e	0.93	2.77	3.642	156
6				
C(17)–H(17)⋯Cl(2) ^f	0.93	2.86	3.519	129
C(28)–H(28)⋯O(2) ^g	0.93	2.64	3.419	142
C(30)–H(30)⋯Cl(1) ^h	0.93	2.73	3.611	158

^a 2 – x, 1 – y, 1 – z.

^b 1 – x, 1/2 + y, 1/2 – z.

^c 2 – x, –1/2 + y, 1/2 – z.

^d 1.5 – x, –1/2 + y, 1/2 – z.

^e 2 – x, 1 – y, 1 – z.

^f x, y, –1 + z.

^g x, 1 + y, –1 + z.

^h –x, 1 – y, 1 – z.

Cl2, Ru-(η^3 ; η^3 -C₁₀H₁₄)/Rh-(η^4 -C₈H₁₂) bonding, envelope plots of some relevant molecular orbitals of **3** and **6** are shown in Fig. S14 and Fig. 8.

3. Conclusion

In this work we have described the syntheses, spectral and structural characterization of the complexes with general formulations [$(\eta^3$; η^3 -C₁₀H₁₆)RuCl₂(L)] (L = CPI, **1**; NOPI, **2**; FPI, **3**; HPI, **4**) and [$(\eta^4$ -C₈H₁₂)RhCl(L)] (L = CPI, **5**; NOPI, **6**; FPI, **7**; HPI, **8**) based on imidazolyl ligands. Structural studies supported our earlier viewpoint that the imidazole containing ligands 1-(4-cyanophenyl)imidazole (CPI), 1-(4-nitrophenyl)imidazole (NOPI), 1-(4-formylphenyl)imidazole (FPI) and 1-(4-hydroxyphenyl)imidazole (HPI) interact with the metal centre through N atom of the imidazole ring. Further, it has been shown that a change in the functional groups on phenyl ring results in a significant change in the properties, which is supported by spectroscopic studies and DFT calculations.

4. Experimental section

4.1. Reagents

All the reagents used were as received without further purifications. Solvents were dried and distilled following the standard literature procedures [54]. Isoprene, 1,5-cyclooctadiene, hydrated rhodium(III) chloride, ruthenium(III) chloride, imidazole, 1-(4-hydroxyphenyl)imidazole (HPI) (all Aldrich) were used as received. The ligands 1-(4-cyanophenyl)imidazole (CPI) [31], 1-(4-nitrophenyl)imidazole (NOPI) [34] and 1-(4-formylphenyl)imidazole (FPI) [35] and precursor complexes [$(\eta^3$; η^3 -C₁₀H₁₆)Ru(μ -Cl)Cl₂] [38] and [$(\eta^4$ -C₈H₁₂)Rh(μ -Cl)Cl₂] [39] were prepared and purified following the literature procedures. C, H and N analyses on the complexes were performed on an Exter CE-440 CHN Analyzer. IR and electronic absorption spectra were recorded on a Perkin Elmer-577 and Shimadzu-UV 1700 spectrophotometers, respectively. ¹H NMR spectra of the complexes in *d*-chloroform at 298 K using TMS as an internal reference were recorded on a JEOL AL 300 FT-NMR machine.

4.1.1. Synthesis of [$(\eta^3$; η^3 -C₁₀H₁₆)RuCl₂(CPI)] (**1**)

CPI (85 mg, 0.5 mmol) was added to a solution of [$(\eta^3$; η^3 -C₁₀H₁₆)Ru(μ -Cl)Cl₂] (154 mg, 0.25 mmol) in dichloromethane

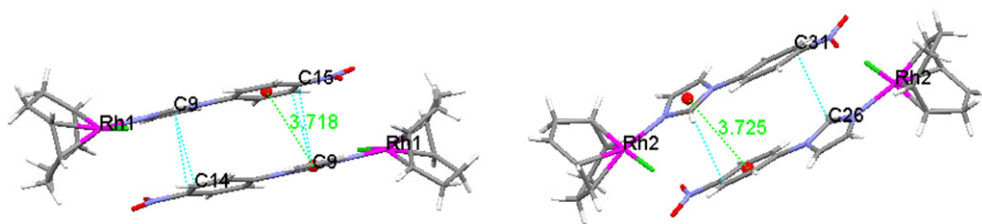


Fig. 6. π - π stacking interactions in **6**.

(15 ml) and stirred at room temperature. After 5 h. it was filtered through celite to remove any solid impurities and the filtrate was evaporated to dryness under reduced pressure. The orange yellow powder thus obtained was extracted with dichloromethane and filtered. The dichloromethane extract was layered with diethyl ether and left for slow crystallization. After a couple of days, shiny golden crystals appeared. These were separated, washed with diethyl ether and dried under vacuum. Yield: 203 mg, 85%. Microanalytical data: $C_{20}H_{23}N_3Cl_2Ru$, requires: C, 50.32; H, 4.86; N, 8.80. Found C, 49.87; H, 4.92; N, 8.65%. 1H NMR ($CDCl_3$, δ ppm): 2.40 (s, 6H of CH_3), 3.10 (m, 4H of CH_2), 4.42 (s, 2H of CH_2 allylic), 4.60 (s, 2H of CH_2 allylic), 5.23 (m, 2H of CH), 7.40 (s, 1H), 7.57 (d, 2H, $J = 7.2$ Hz), 7.83 (d, 2H, $J = 7.2$ Hz), 7.91 (s, 1H), 8.72 (s, 1H). $^{13}C\{^1H\}$ NMR ($CDCl_3$, δ ppm): 21.10 (CH_3), 36.89 (C4 and C5), 77.08 (C1 and C8), 95.25 (C3 and C6), 133.45 (C2 and C7), 112.14 (CN), 117.65, 118.10, 121.38, 128.69, 134.08, 138.37, 139.19.

4.1.2. Synthesis of $[(\eta^3;\eta^3-C_{10}H_{16})RuCl_2(NOPI)]$ (**2**)

It was prepared following the above procedure **1** except that NOPI (95 mg, 0.5 mmol) was used in place of CPI. Yield: 201 mg, 81%. Microanalytical data: $C_{19}H_{23}N_3O_2Cl_2Ru$, requires: C, 45.88; H, 4.66; N, 8.45. Found C, 45.45; H, 4.53; N, 8.03%. 1H NMR ($CDCl_3$, δ ppm): 2.40 (s, 3H of CH_3), 2.48 (m, 3H of CH_3), 3.07 (m, 4H of CH_2), 4.43 (s, 2H CH_2 allylic), 4.60 (s, 2H CH_2 allylic), 5.23 (m, 1H CH) 5.30

(s, 1H CH), 7.43 (s, 1H), 7.62 (d, 2H $J = 9$ Hz), 7.94 (s, 1H), 8.40 (d, 2H $J = 9$ Hz), 8.76 (s, 1H). $^{13}C\{^1H\}$ NMR ($CDCl_3$, δ ppm): 21.12 (CH_3), 36.86 (C4 and C5), 77.10 (C1 and C8), 95.24 (C3 and C6), 133.46 (C2 and C7), 117.65, 121.38, 125.82, 129.69, 139.08, 141.03, 146.92.

4.1.3. Synthesis of $[(\eta^3;\eta^3-C_{10}H_{16})RuCl_2(FPI)]$ (**3**)

It was prepared following the above procedure **1** using FPI (86 mg, 0.5 mmol) in place of CPI. Yield: 187 mg, 78%. Microanalytical data: $C_{20}H_{24}N_2Cl_2ORu$, requires: C, 50.00, H, 5.04, N, 5.83. Found C, 49.72, H, 5.28, N, 5.44. 1H NMR ($CDCl_3$, δ ppm): 2.39 (s, 6H of CH_3), 3.08 (m, 2H of CH_2), 4.41 (s, 3H of CH_2 allylic), 4.58 (s, 3H of CH_2 allylic), 5.24 (m, 2H of CH) 7.43 (s, 1H), 7.61 (d, 2H, $J = 6$ Hz), 7.89 (s, 1H), 8.02 (s, 7.89), 8.07 (d, 2H $J = 12.6$ Hz), 8.73 (s, 1H) 10.06 (s, 1H). $^{13}C\{^1H\}$ NMR ($CDCl_3$, δ ppm): 21.12 (CH_3), 36.86 (C4 and C5), 77.80 (C1 and C8), 95.24 (C3 and C6), 133.45 (C2 and C7), 116.89, 118.24, 121.78, 128.84, 136.54, 139.25, 140.67.

4.1.4. Synthesis of $[(\eta^3;\eta^3-C_{10}H_{16})RuCl_2(HPI)]$ (**4**)

It was prepared following the above procedure for **1**, except that HPI (74 mg, 0.5 mmol) was used in place of CPI. Yield: 166 mg, 71%. Microanalytical data: $C_{19}H_{24}N_2Cl_2ORu$, requires: C, 48.72; H, 5.16; N, 9.31. Found C, 48.79; H, 5.26; N, 9.30%. 1H NMR ($CDCl_3$, δ ppm): 2.40 (s, 6H of CH_3), 3.08 (m, 2H of CH_2), 4.42 (s, 3H of CH_2 allylic), 4.56 (s, 3H of CH_2 allylic), 5.24 (m, 2H of CH), 7.44 (s, 1H), 7.62 (d, 2H,

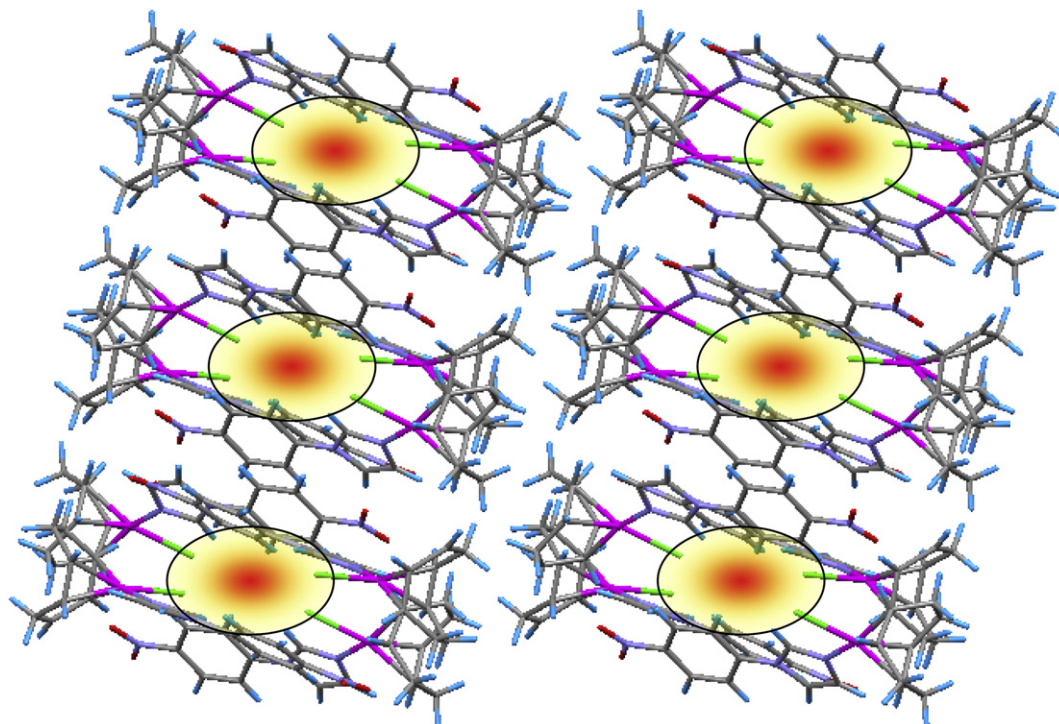
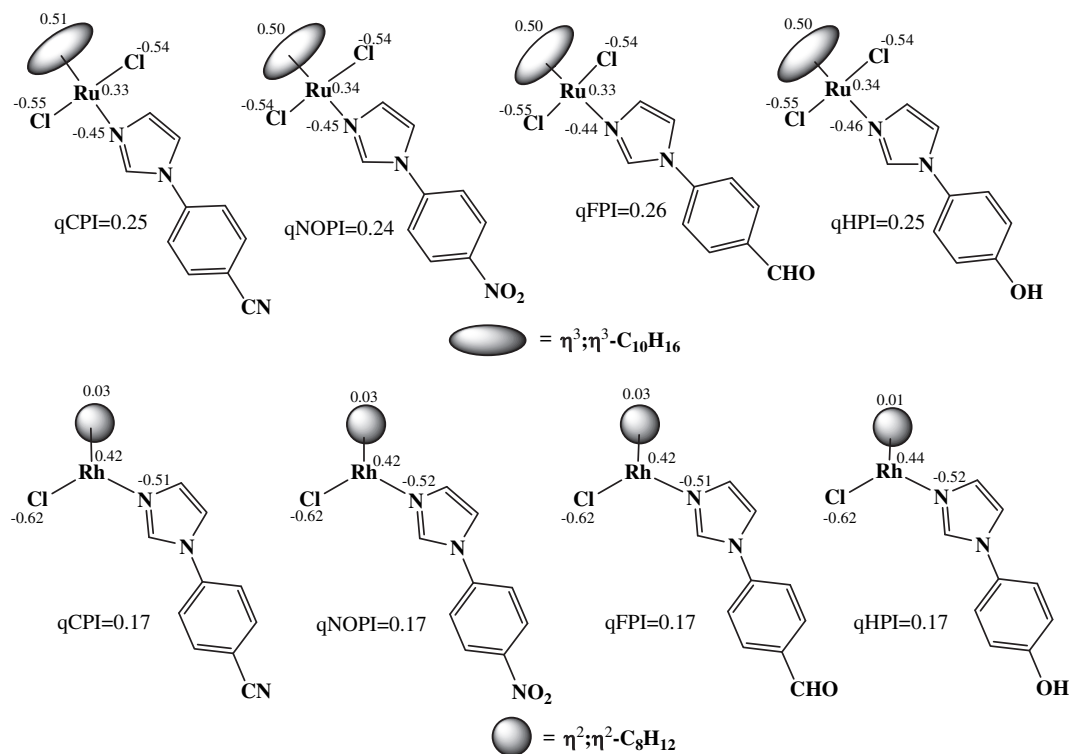


Fig. 7. Cavity resulting through weak interactions in complex **6**.



Scheme 2. Natural charge distribution in complexes 1–8.

J, 6 Hz), 7.89 (s, 1H), 8.02 (s, 7.89), 8.06 (d, 2H, $J = 12.6$ Hz), 8.75 (s, 1H), 10.56 (s, 1H). $^{13}\text{C}\{^1\text{H}\}$ NMR (CDCl_3 , δ ppm): 21.12 (CH₃), 36.79 (C4 and C5), 77.92 (C1 and C8), 95.24 (C3 and C6), 133.49 (C2 and C7), 117.70, 118.12, 121.46, 129.89, 135.69, 139.08, 141.03.

4.1.5. Synthesis of $[(\eta^4\text{-C}_8\text{H}_{12})\text{RhCl}(\text{CPI})]$ (**5**)

A solution of $[(\eta^4\text{-C}_8\text{H}_{12})\text{Rh}(\mu\text{-Cl})\text{Cl}_2]$ (123 mg, 0.25 mmol) in dichloromethane (15 ml) was treated with CPI (85 mg, 0.5 mmol) and stirred for 5 h at r.t. It was filtered through celite and evaporated to dryness under reduced pressure. The orange yellow powder thus obtained was extracted with dichloromethane, layered with diethyl ether and left for slow crystallization. After a couple of days shiny golden crystals separated. These were separated, washed with diethyl ether and dried in air. Yield 173 mg 83%. Microanalytical data: $\text{C}_{18}\text{H}_{19}\text{N}_3\text{ClRh}$, requires: C, 50.00; H, 4.61; N, 10.11%. Found C, 49.85; H, 4.68; N, 9.98%. ^1H NMR (CDCl_3 , δ ppm): 1.86 (d, 4H, $J = 7.2$ Hz CH₂ of cod), 2.51 (s, 4H CH₂ of cod), 4.55 (broad, 4H CH of cod), 6.97 (s, 1H), 7.52 (d, 2H, $J = 7.5$ Hz), 7.82 (d, 2H, $J = 7.8$), 8.71 (s, 1H). $^{13}\text{C}\{^1\text{H}\}$ NMR (CDCl_3 , δ ppm): 30.748 (CH₂ of cod), 79.63 (CH of cod), 112.26 (CN), 117.37, 118.10, 121.85, 128.37, 134.16, 138.23, 139.19. UV–vis. $\{\text{CH}_2\text{Cl}_2, \lambda_{\text{nm}} (\epsilon)\}$: 618 (108), 374 (6×10^2), 292 (7.88×10^3).

4.1.6. Synthesis of $[(\eta^4\text{-C}_8\text{H}_{12})\text{RhCl}(\text{NOPI})]$ (**6**)

It was prepared following the above procedure for **5** using NOPI (74 mg, 0.5) in place of CPI Yield: 176 mg, 81%. Microanalytical data: $\text{C}_{17}\text{H}_{19}\text{N}_3\text{ClO}_2\text{Rh}$; requires: C, 46.86; H, 4.40; N, 9.64%. Found C, 46.74; H, 4.38; N, 9.56%. ^1H NMR (CDCl_3 , δ ppm): 1.86 (d, 4H, $J = 8.1$ Hz CH₂ of cod), 2.49 (s, 4H CH₂ of cod), 4.34 (broad, 4H CH of cod), 7.00 (s, 1H), 7.58 (d, 2H, $J = 9$ Hz), 8.39 (d, 2H, $J = 8.7$ Hz), 8.72 (s, 1H). $^{13}\text{C}\{^1\text{H}\}$ NMR (CDCl_3 , δ ppm): 30.75 (CH₂ of cod), 79.62 (CH of cod) 118.20, 121.67, 125.75, 125.36, 128.36, 138.32, 140.63, 146.96. UV–vis. $\{\text{CH}_2\text{Cl}_2, \lambda_{\text{nm}} (\epsilon)\}$: 597 (112), 377 (4.72×10^2), 261 (8.78×10^3).

4.1.7. Synthesis of $[(\eta^4\text{-C}_8\text{H}_{12})\text{RhCl}(\text{FPI})]$ (**7**)

It was prepared following the above procedure for **5** except that FPI (86 mg, 0.5 mmol) was used in place of CPI. Yield: 167 mg, 80%. Microanalytical data: $\text{C}_{18}\text{H}_{20}\text{N}_2\text{ClORh}$, requires: C, 51.63; H, 4.81; N, 6.69%. Found C, 51.46; H, 4.86; N, 6.55%. ^1H NMR (CDCl_3 , δ ppm): 1.83 (d, 4H, $J = 7.5$ Hz CH₂ of cod), 2.49 (s, 4H, CH₂ of cod) 4.27 (broad, 4H, CH of cod), 6.97 (s, 1H), 7.57 (d, 2H, $J = 8.1$ Hz), 8.03 (d, 2H, $J = 8.1$ Hz), 8.69 (s, 1H), 10.05 (s, 1H). $^{13}\text{C}\{^1\text{H}\}$ NMR (CDCl_3 , δ ppm): 30.75 (CH₂ of cod), 79.62 (CH of cod) 116.85, 118.25, 121.80, 128.85, 136.54, 139.25, 140.66. UV–vis. $\{\text{CH}_2\text{Cl}_2, \lambda_{\text{nm}} (\epsilon)\}$: 605 (105), 376 (8.26×10^2), 288 (9.13×10^3).

4.1.8. Synthesis of $[(\eta^4\text{-C}_8\text{H}_{12})\text{RhCl}(\text{HPI})]$ (**8**)

It was prepared following the above procedure adopted for **5** except HPI (74 mg, 0.5 mmol) was used in place of CPI. Yield: 159 mg, 78%. Microanalytical data: $\text{C}_{17}\text{H}_{20}\text{N}_2\text{ClORh}$ requires: C, 50.20; H, 4.96; N, 6.89% Found: C, 50.12; H, 4.88; N, 6.52%. ^1H NMR (CDCl_3 , δ ppm): 1.84 (d, 4H, $J = 7.5$ Hz CH₂ of cod), 2.50 (s, 4H, CH₂ of cod), 4.25 (broad, 4H, CH of cod), 6.95 (s, 1H), 7.57 (d, 2H, $J = 8.1$ Hz), 8.02 (d, 2H, $J = 8.1$), 8.67 (s, 1H), 10.50 (s, 1H). $^{13}\text{C}\{^1\text{H}\}$ NMR (CDCl_3 , δ ppm): 30.75 (CH₂ of cod), 79.64 (CH of cod) 117.70, 118.15, 121.50, 129.88, 135.69, 139.12, 141.08. UV–vis. $\{\text{CH}_2\text{Cl}_2, \lambda_{\text{nm}} (\epsilon)\}$: 610 (102), 380 (8.95×10^2), 291 (9.08×10^3).

4.2. Crystallographic data

Crystals suitable for single crystal X-ray diffraction analyses for **2**, **5** and **6** were obtained by slow diffusion from dichloromethane/diethyl ether. X-ray data on **2**, **5** and **6** were collected on a R-AXIS RAPID II diffractometer at room temperature with Mo-K α radiation ($\lambda = 0.71073$ Å) at the single crystal X-diffraction centre of National Institute of Advanced Industrial Science and Technology (AIST), Osaka, Japan. Structures were solved by direct methods (SHELXS 97) and refined by full-matrix least squares calculations on F^2

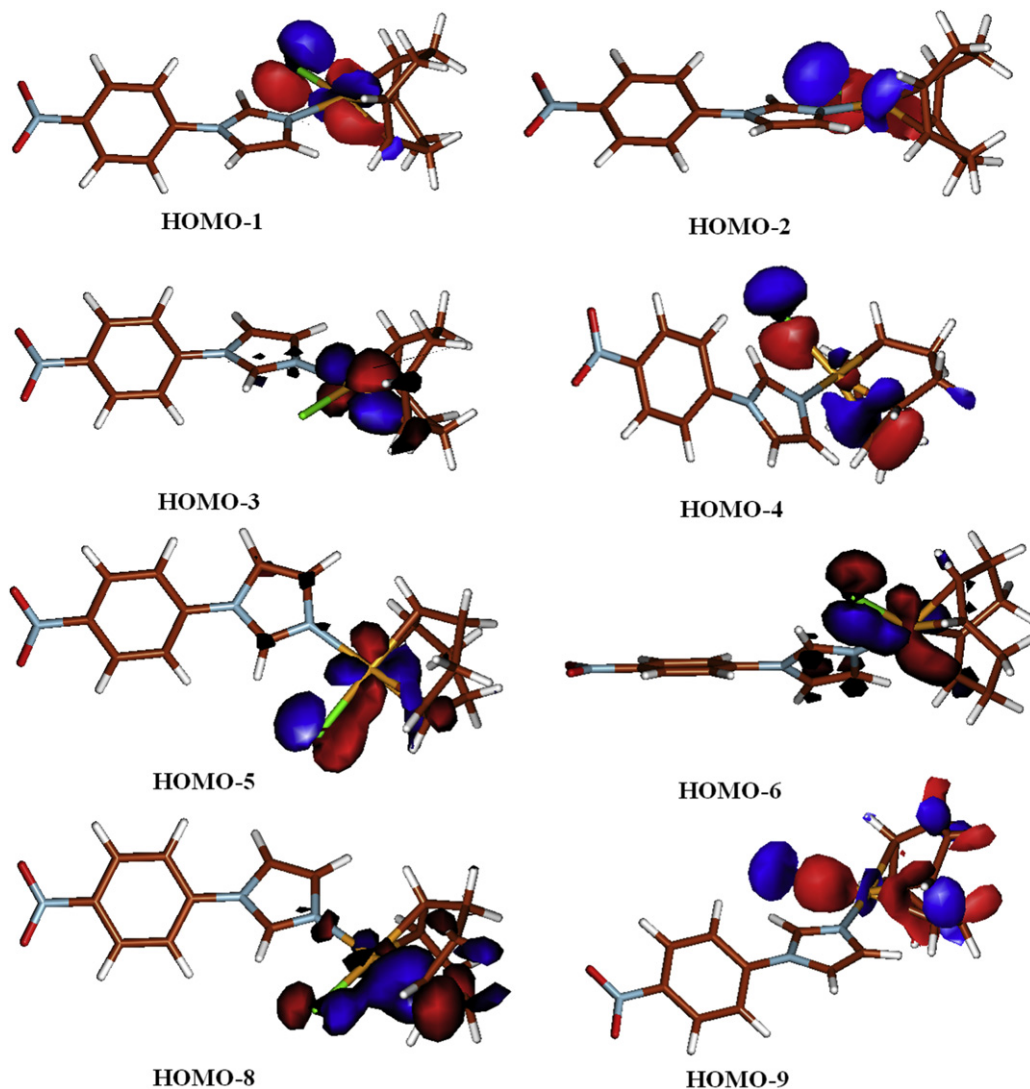


Fig. 8. Bonding orbitals of complex 6.

(SHELX 97) [55]. All the non-H atoms were treated anisotropically. H-atoms attached to the carbon were included as fixed contribution and were geometrically calculated and refined using the SHELX riding model [56]. These data can be obtained free of charge via <http://www.ccdc.cam.ac.uk/conts/retrieving.html> (or from the CCDC, 12 Union Road, Cambridge CB2 1EZ, UK; Fax: +44-1223-336033; E-mail: deposit@ccdc.cam.ac.uk).

Complex 2. Formula = $C_{38}H_{42}Cl_4N_6O_4Ru_2$, Mr = 990.72, Monoclinic, Space group $P21/c$, a (Å) = 13.628(3), b (Å) = 15.203(3), c (Å) = 19.841(4), α (°) = 90.00, β (°) = 102.08(3), γ (°) = 90.00, V (Å³) = 4020.0(14), $Z = 4$, D_c ($Mg\ m^{-3}$) = 1.637, T (K) = 293(2), λ (Å) = 0.71073, R (all) = 0.0435, R [$I > 2\sigma(I)$] = 0.0306, $wR2$ = 0.0898, $wR2$ [$I > 2\sigma(I)$] = 0.0847, $Goof$ = 1.060.

Complex 5. Formula = $C_{18}H_{17}ClN_3Rh$, Mr = 413.71, Monoclinic, Space group $P21/n$, a (Å) = 15.260(3), b (Å) = 7.8964(16), c (Å) = 15.265(3), α (°) = 90.00, β (°) = 112.95(3), γ (°) = 90.00, V (Å³) = 1693.8(6), $Z = 4$, D_c ($Mg\ m^{-3}$) = 1.622, T (K) = 293(2), λ (Å) = 0.71073, R (all) = 0.0378, R [$I > 2\sigma(I)$] = 0.0302, $wR2$ = 0.0988, $wR2$ [$I > 2\sigma(I)$] = 0.0907, $Goof$ = 1.064.

Complex 6. Formula = $C_{34}H_{37}Cl_2N_6O_4Rh_2$, Mr = 870.42, Triclinic, Space group $P-1$, a (Å) = 7.3961(15), b (Å) = 14.416(3), c (Å) = 16.847(3), α (°) = 103.08(3), β (°) = 101.11(3), γ (°) = 91.84

(3), V (Å³) = 1711.4(6), $Z = 2$, D_c ($Mg\ m^{-3}$) = 1.689, T (K) = 293(2), λ (Å) = 0.71073, R (all) = 0.0753, R [$I > 2\sigma(I)$] = 0.0370, $wR2$ = 0.0830, $wR2$ [$I > 2\sigma(I)$] = 0.0654, $Goof$ = 1.061.

4.3. Computational methods

Calculations were performed using hybrid B3LYP density functional method which uses Becke's 3-parameter nonlocal exchange functional mixed with the exact (Hartree-Fock) exchange functional and Lee-Yang-Parr's nonlocal correlation functional [57,58]. Geometries of the complexes were optimized without any symmetry restriction with standard 6-31G** basis sets for N, C, H, O and Cl elements and LANL2DZ for Ru and Rh which combines quasi-relativistic effective core potentials with a valence double-basis set [59–63]. Frequency calculations were performed to determine whether the optimized geometries are minima on the potential energy surface. The electronic structures of complexes were examined by natural charges at each atom computed using Kohn–Sham orbitals obtained from DFT calculations [64] using 6-311G(d) basis sets for N, C, H, O and Cl elements and LANL2DZ for Ru and Rh elements. The calculations carried out using the programme the GAUSSIAN03 [65].

Acknowledgement

Thanks are due to the Department of Science and Technology, New Delhi, India for providing financial assistance through Scheme No. SR/S1/IC-15/2006. RKG acknowledges the Council of Scientific and Industrial Research (CSIR), New Delhi, India for awarding a Junior Research Fellowship (09/013(0210)/2009-EMR-I). We are also thankful to the Head, Department of Chemistry, Banaras Hindu University, Varanasi (U.P.) India and National Institute of Advanced Industrial Science and Technology (AIST), Osaka, Japan for extending facilities.

Appendix. Supplementary information

CCDC-743000 (2), 743002 (5) and 743001 (6) contain the supplementary crystallographic data for this paper. In addition, Tables S1 and S2 and Figs. S1–S14 containing ¹³C NMR Spectra, motifs resulting from various weak interactions and optimized molecular structures and molecular orbitals. These data can be obtained free of charge from The Cambridge Crystallographic Data Centre via www.ccdc.cam.ac.uk/data_request/cif.

References

- [1] L. Porri, M.C. Gallazzi, A. Colombo, G. Allegra, *Tetrahedron Lett.* 47 (1965) 4187.
- [2] L. Porri, G. Allegra, *Acta Crystallogr. B* 27 (1971) 1653.
- [3] M.A. Bennett, M.I. Bruce, T.W. Matheson, in: G. Wilkinson, F.G.A. Stone, E. W. Abel (Eds.), *Comprehensive Organometallic Chemistry*, Ser. 4, Pergamon Press, Oxford, U.K, 1982, p. 796.
- [4] H. Le Bozec, D. Touchard, P.H. Dixneuf, *Adv. Organomet. Chem.* 29 (1989) 163.
- [5] E. Wong, C.M. Giandomenico, *Chem. Rev.* 99 (1999) 2451.
- [6] C.E. Housecroft, in: J.A. McCleverty, T.J. Meyer (Eds.), *Comprehensive Coordination Chemistry II*, Pergamon Press, Oxford, U.K, 2005, p. 555.
- [7] T. Naota, H. Takaya, S.E. Murahashi, *Chem. Rev.* 98 (1998) 2599.
- [8] C. Bruneau, P.H. Dixneuf, *Ruthenium Catalysis and Fine Chemistry*. Springer, Berlin, 2004, pp. 45–79.
- [9] L. Porri, M.C. Gallazzi, A. Colombo, G. Allegra, *Tetrahedron Lett.* 47 (1965) 4187.
- [10] D.N. Cox, R. Roulet, *Inorg. Chem.* 29 (1990) 1360.
- [11] R.A. Head, J.F. Nixon, J.R. Swain, C.M. Woodard, *J. Organomet. Chem.* 76 (1974) 93.
- [12] G. Ertl, H. Knozinger, J. Weitkamp (Eds.), *Handbook of Heterogeneous Catalysis*, Wiley-VCH, Weinheim, 1997.
- [13] H.U. Blaser, H. Steiner, M. Studer, in: M. Beller, C. Bolm (Eds.), *Transition Metals for Organic Synthesis*, vol. 2, Wiley-VCH, Weinheim, 1998 Chapter 1.2.
- [14] W.A. Herrmann, *Angew. Chem. Int. Ed.* 27 (1988) 1297.
- [15] C. Che, W. Cheng, W. Leung, T.C.W. Mak, *J. Chem. Soc., Chem. Commun.* (1987) 418.
- [16] J.M. Lehn, *Supramolecular Chemistry*. VCH, Weinheim, Germany, 1995, p. 298.
- [17] S.I. Stupp, P.V. Braun, *Science* 277 (1997) 1242.
- [18] U.B. Sleytr, P. Messner, D. Pum, M. Sara, *Angew. Chem. Int. Ed.* 38 (1999) 1034.
- [19] R. Oesterbacka, C.P. An, X.M. Jiang, Z.V. Vardeny, *Science* 287 (2000) 839.
- [20] G.R. Desiraju, *Angew. Chem. Int. Ed.* 34 (1995) 2311.
- [21] J. Kim, B. Chen, T.M. Reineke, H. Li, M. Eddaoudi, D.B. Moler, M. O'Keeffe, O. M. Yaghi, *J. Am. Chem. Soc.* 123 (2001) 8239.
- [22] R.J. Sundberg, R.B. Martin, *Chem. Rev.* 74 (1974) 471.
- [23] N. Masciocchi, G.A. Ardizzoia, G. LaMonica, A. Maspero, S. Galli, A. Sironi, *Inorg. Chem.* 40 (2001) 6983.
- [24] N. Masciocchi, F. Castelli, P.M. Forster, M.M. Tafoya, A.K. Cheetham, *Inorg. Chem.* 42 (2003) 6147.
- [25] S.J. Rettig, A. Storr, D.A. Summers, R.C. Thompson, J. Trotter, *J. Am. Chem. Soc.* 119 (1997) 8675.
- [26] J. He, J.-X. Zhang, G.-P. Tan, Y.-G. Yin, D. Zhang, M.-H. Hu, *Cryst. Growth Des.* 7 (2007) 1508.
- [27] K.R. Dunbar, R.A. Heintz, *Progress in Inorganic Chemistry*, vol. 45, John Wiley & Sons, New York, 1997, p. 283.
- [28] D. Ramprasad, G.P. Pez, B.H. Toby, T.J. Markley, R.M. Pearlstein, *J. Am. Chem. Soc.* 117 (1995) 10694.
- [29] O. Sato, Z.Z. Gu, H. Etoh, J. Ichiyana, T. Iyoda, A. Fujishima, K. Hashimoto, *Chem. Lett.* (1997) 37.
- [30] G.B. Less, J.W. Kampf, P.G. Rasmussen, *Inorg. Chem.* 43 (2004) 4897.
- [31] A. Hatzidimitriou, A. Gourdon, J. Devillers, J.-P. Launay, E. Mena, E. Mouyal, *Inorg. Chem.* 35 (1996) 2212.
- [32] S.K. Singh, M. Trivedi, M. Chandra, A.N. Sahay, D.S. Pandey, *Inorg. Chem.* 43 (2004) 26.
- [33] S.K. Singh, M. Trivedi, M. Chandra, D.S. Pandey, *J. Organomet. Chem.* 690 (2005) 647.
- [34] P. Lo Meo, F. D'Anna, S. Riel, M. Gruttadauria, R. Noto, *Tetrahedron* 63 (2007) 9163.
- [35] Z.-Q. Liang, C.-X. Wang, J.-X. Yang, H.-W. Gao, Y.-P. Tian, X.-T. Tao, M.-H. Jiang, *New J. Chem.* 31 (2007) 906.
- [36] S.K. Singh, S. Joshi, A.R. Singh, J.K. Saxena, D.S. Pandey, *Inorg. Chem.* 46 (2007) 10869.
- [37] A.K. Singh, M. Yadav, P. Kumar, S.K. Singh, S. Sunkari, D.S. Pandey, *J. Mol. Struct.* 935 (2009) 1.
- [38] G. Toerien, P.H. von Rooyen, *J. Chem. Soc. Dalton Trans.* (1991) 1563.
- [39] G. Giordano, R.H. Crabtree, *Inorg. Synth.* 28 (1990) 88.
- [40] Jaishela Rajput, Alan T. Hutton, John R. Moss, Hong Su, Christopher Imrie, *J. Organomet. Chem.* 691 (2006) 4573.
- [41] J.E. Huheey, E.A. Keiter, R.L. Keiter, O.K. Medhi, *Inorganic Chemistry; Principles of Structure and Reactivity*. Pearson Education, 2006, pp. 501 and references therein.
- [42] F. Shriver, P.W. Atkins, C.H. Langford (Eds.), *Inorg. Chem.*, Oxford University Press, Oxford, 1994, p. 581.
- [43] A.N. Sahay, D.S. Pandey, M.G. Walawalkar, *J. Organomet. Chem.* 613 (2000) 250.
- [44] J.A. Kudak, A.T. Poulos, J.A. Ibers, *J. Organomet. Chem.* 127 (1977) 245.
- [45] A. Colombo, G. Allegra, *Acta Crystallogr. Sect. B* 27 (1971) 1653.
- [46] D.N. Cox, R.W.H. Small, R. Roulet, *J. Chem. Soc. Dalton Trans.* (1991) 2013.
- [47] S.O. Sorwiere, G.J. Palenik, *Organometallics* 10 (1991) 12203.
- [48] J.W. Steed, D.A. Tocher, *J. Organomet. Chem.* 412 (1991) 393.
- [49] M.A. Bennett, G.B. Robertson, A.K. Smith, *J. Organomet. Chem.* 43 (1972) C41.
- [50] M.R.J. Elsegood, D.A. Tocher, *Polyhedron* 14 (1995) 3147.
- [51] C. Menendez, D. Morales, J. Perez, V. Riera, D. Miguel, *Organometallics* 20 (2001) 2775.
- [52] A.K. Singh, P. Kumar, M. Yadav, D.S. Pandey, *J. Organomet. Chem.* 695 (2010) 567.
- [53] <http://www.ccdc.cam.ac.uk/products/csd/radii/table.php4>.
- [54] D.D. Perrin, W.L.F. Armango, D.R. Perrin, *Purification of laboratory Chemicals*. Pergamon, Oxford, UK, 1986.
- [55] G.M. Sheldrick, SHELXL 97, Programme for Refining Crystal Structures. University of Göttingen, Germany, 1997, p. 67.
- [56] G.M. Sheldrick, SHELXS 97, Programme for the Solution of Crystal Structures. University of Göttingen, Germany, 1990.
- [57] A.D. Becke, *J. Chem. Phys.* 98 (1993) 5648.
- [58] C.T. Lee, W.T. Yang, R.G. Parr, *Phys. Rev. B: Condens. Matter Mater. Phys.* 37 (1988) 785.
- [59] R. Krishnan, J.S. Binkley, R. Seeger, J.A. Pople, *J. Chem. Phys.* 72 (1980) 650.
- [60] A.D. McClean, G.S. Chandler, *J. Chem. Phys.* 72 (1980) 5639.
- [61] P. Hay, W.R. Wadt, *J. Chem. Phys.* 82 (1985) 270.
- [62] W.R. Wadt, P. Hay, *J. Chem. Phys.* 82 (1985) 284.
- [63] P. Hay, W.R. Wadt, *J. Chem. Phys.* 82 (1985) 299.
- [64] W. Kohn, L.J. Sham, *Phys. Rev.* 140 (1965) 1133.
- [65] M.J. Frisch, G.W. Trucks, H.B. Schlegel, G.E. Scuseria, M.A. Robb, J. R. Cheeseman, J.A. Montgomery Jr., T. Vreven, K.N. Kudin, J.C. Burant, J. M. Millam, S.S. Iyengar, J. Tomasi, V. Barone, B. Mennucci, M. Cossi, G. Scalmani, N. Rega, G.A. Petersson, H. Nakatsuji, M. Hada, M. Ehara, K. Toyota, R. Fukuda, J. Hasegawa, M. Ishida, T. Nakajima, Y. Honda, O. Kitao, H. Nakai, M. Klene, X. Li, J.E. Knox, H.P. Hratchian, J.B. Cross, V. Bakken, C. Adamo, J. Jaramillo, R. Gomperts, R.E. Stratmann, O. Yazyev, A.J. Austin, R. Cammi, C. Pomelli, J. Ochterski, P.Y. Ayala, K. Morokuma, G.A. Voth, P. Salvador, J.J. Dannenberg, V.G. Zakrzewski, S. Dapprich, A.D. Daniels, M. C. Strain, O. Farkas, D.K. Malick, A.D. Rabuck, K. Raghavachari, J.B. Foresman, J. V. Ortiz, Q. Cui, A.G. Baboul, S. Clifford, J. Cioslowski, B.B. Stefanov, G. Liu, A. Liashenko, P. Piskorz, I. Komaromi, R.L. Martin, D.J. Fox, T. Keith, M.A. Al-Laham, C.Y. Peng, A. Nanayakkara, M. Challacombe, P.M.W. Gill, B.G. Johnson, W. Chen, M.W. Wong, C. Gonzalez, J.A. Pople, GAUSSIAN 03 (Revision D.01). Gaussian, Inc., Wallingford, CT, 2004.